## Laboratory Demonstration of an Infrared-to-Visible Up-Conversion Interferometer for Spatial Coherence Analysis

S. Brustlein, L. Del Rio, A. Tonello, L. Delage, and F. Reynaud\*

XLIM Département Photonique, UMR CNRS 6172, 123 Avenue A. Thomas, 87060 Limoges Cedex, France

## H. Herrmann and W. Sohler

Universität Paderborn, Angewandte Physik, Warburger Strasse 100-33098 Paderborn, Germany (Received 10 January 2008; published 16 April 2008)

We experimentally demonstrate the possibility of retrieving the spatial coherence of an infrared source by using an up-conversion interferometer. Sum-frequency generation in Ti-diffused periodically poled lithium-niobate waveguides in both arms of the interferometer is used to convert the infrared into the visible domain. The fringe contrast of the interference pattern in the visible domain permits us to resolve the spatial separation of two uncorrelated pointlike infrared sources, which simulate a binary star. The validity of these measurements is confirmed through a simultaneous comparison with a reference interferometer working in the infrared domain.

DOI: 10.1103/PhysRevLett.100.153903 PACS numbers: 42.65.Ky, 42.25.Kb

In the last five decades, different optical techniques have been proposed to improve the angular resolution of astronomical instruments [1]. These techniques have been inspired by previous work since the beginning of the 20th century. We summarize the basic schemes of imaging interferometry of infrared radiation (IR) in Fig. 1. The widely used scheme is an interferometer in which the optical signals are mixed before detection [2] as illustrated in Fig. 1(a). In a similar way, the spatial coherence can be analyzed after an optical to electric conversion in appropriate photodetectors (IR detectors) followed by a subsequent electronic cross correlation. This can either be done by direct [Fig. 1(b)] [3] or by heterodyne detection [Fig. 1(c)] [4]. In the latter case the optical signals are mixed with a local optical oscillator which strongly improves the sensitivity. However, in both cases highly sensitive ultrafast photodetectors (with nano- or picosecond response time) are required, which are not available for the infrared region.

In this Letter, we propose and demonstrate a novel scheme as shown in Fig. 1(d). In contrast to the conventional interferometric scheme [Fig. 1(a)], our new solution involves an up-conversion of the infrared radiation (IR) into the visible domain. This is obtained using all-optical wavelength converters in both arms of the interferometer. Our scope is to demonstrate the applicability of such an upconversion interferometer for high resolution imaging. Therefore, we experimentally prove the spatial coherence of a given infrared source to be transferred by the wavelength conversion process. Recent experiments on fiber transmission systems have already shown the compatibility of wavelength conversion in periodically poled lithiumniobate (PPLN) waveguides with high-bit rate modulation formats based on phase-shift keying [5]. In that case, the phase difference between adjacent pulses has discrete values of type 0 or  $\pi$ . In our experiment, the phase difference can be several times larger than  $2\pi$  and the image information signal is carried by the fringe contrast function. An interferometer which includes frequency down-conversion in gases has already been proposed in Ref. [6]. In astro-

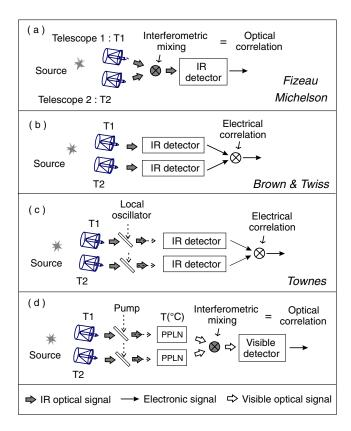


FIG. 1 (color online). Basic schemes of IR imaging interferometry with telescopes T1 and T2. (a) Direct detection interferometry. (b) Intensity interferometry with direct detection. (c) Intensity interferometry with heterodyne detection. (d) Novel up-conversion interferometer.

nomical imaging the principal restrictions come from the low level of signal power at the IR wavelengths and from the background noise. Additionally, in stellar interferometry one needs to combine the signal from at least two telescopes. This can be done in practice by using single mode optical fibers [7]. Several applications based on sumfrequency generation (SFG) processes have been developed in astronomy [8,9] and quantum communications [10–12]. To our knowledge, no applications of SFG in high resolution imaging by spatial coherence analysis have been reported yet.

To discuss the potential of such up-conversion interferometers let us first recall some basics on indirect imaging through interferometry. Consider a spatially incoherent object emitting quasimonochromatic light, centered around a carrier wavelength  $\lambda_{\rm IR}$ , and having an angular intensity distribution of  $O(\theta)$  ( $\theta$  is the angular position; see Fig. 2). For ease of discussion, in what follows we will reduce our analysis to only one spatial dimension. The intensity distribution  $O(\theta)$  illuminates two distinct telescopes spaced by a distance x. The interference of the optical fields from the two telescopes generates a fringe pattern which is modulated by the corresponding complex visibility

$$V(\xi) = \frac{1}{I} \int_{\text{object}} O(\theta) \exp(j2\pi\theta \xi) d\theta \tag{1}$$

where  $\xi = x/\lambda_{\rm IR}$ . Equation (1) resumes the Zernikevan Cittert theorem which connects the fringe visibility with the Fourier transform of the intensity distribution, i.e.,  $V(\xi) = (1/I)\mathcal{F}[O(\theta)]$  (see Ref. [13] for details). Using the up-conversion interferometer we are going to demonstrate that the visibility function is distortionlessly transferred from the infrared domain into the visible domain. Obviously, this brings several advantages: In the visible region, photodetectors have a by far higher sensitivity compared to the best IR detectors, which are very expen-

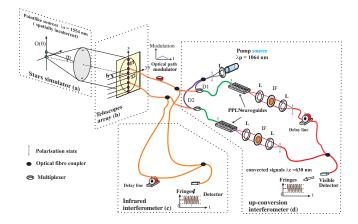


FIG. 2 (color online). Experimental setup. IF: interference filter ( $\lambda = 630 \pm 20$  nm);  $T(^{\circ}\text{C})$ : temperature controller; L: Lens.

sive and need additional cooling systems down to liquid nitrogen temperature or below. For the visible range single photon counting detectors are commercially available with, for instance, a quantum yield of 75% at an operation wavelength of 700 nm. In Ref. [14] an improved detectivity of a low power IR signal at 1.5  $\mu$ m with a wavelength conversion to  $0.7 \mu m$  has been demonstrated. In their experiment, the large quantum yield of the single photon detector largely overcompensates the incomplete power conversion ( - 10 dB efficiency). We expect further advantages from the application of up-conversion interferometers when considering the analysis of far infrared radiations. A frequency conversion from the far to the near infrared domain would open the possibility of extending the use of the telescope fiber link, whose applicability is presently limited to the visible and near IR domain. For instance, a simple intensity conversion of a 10.6 µm signal has been reported in Ref. [15]. The key elements of the upconversion interferometer are the wavelength converters. An efficient conversion even at moderate pump power levels is required. Therefore, waveguide-based integrated optical devices with a tight confinement of the optical waves within a small effective area over a long interaction length are preferred. Low loss Ti-indiffused waveguides in PPLN are well suited for this purpose as long as the signal wavelength is within the transparency range of LiNbO<sub>3</sub>, i.e., below about 5  $\mu$ m. Therefore, we have chosen Ti:PPLN waveguides for our experiments to demonstrate the basic functionalities of the up-conversion interferometer. SFG is used to convert a weak infrared signal at about 1.55  $\mu$ m into the visible (around 630 nm) using a pump wave at 1064 nm.

Our experimental setup, at XLIM, is composed of four main subsystems as shown in Fig. 2. The object is composed of a pair of spatially incoherent point sources acting as a laboratory binary star. In practice we split the optical radiation of a distributed-feedback (DFB) laser source at 1541 nm into two distinct optical fibers by means of a polarization-maintaining (PM) fiber coupler. (PM fibers and components are used throughout the whole setup to guarantee maximum fringe contrast.) The spatial decorrelation of the two secondary sources is ensured by a 500 m long highly birefringent fiber, which is longer than the coherence length of our DFB laser (100 m). The two fiber outputs, acting as incoherent pointlike sources, are located in the focal plane of a collimating lens with a focal length of f = 1900 mm. The corresponding angular separation is  $\theta_0 \sim 14.7 \ \mu \text{rad}$ . The use of such an object is a classical test to validate the imaging capability of an instrument.

To measure the fringe contrast for different values of x, a "telescope array" consisting of eight achromatic doublets (f=10 mm) is used. The lenses are periodically spaced by b=16 mm. The corresponding minimum and maximum spatial frequencies are  $\lambda/(7b)=1.04\times10^4$  rad<sup>-1</sup> and  $\lambda/(b)=8.32\times10^4$  rad<sup>-1</sup>, respectively. This set of

spatial frequencies permits us to observe more than one period of the visibility function of the binary star. The smaller spatial frequency has been selected to satisfy the Nyquist-Shannon sampling criterium.

The light collected by each telescope is then injected into a fiber. The interference of the signals from two telescopes is investigated. To display the fringes, the optical path length in one arm is modulated. We use a triangular modulation function m(t) which generates a linear delay within a half period. A system of PM fiber couplers (splitting ratio 10:1) splits the infrared signals into two paths (see Fig. 2) and routes them to the up-conversion interferometer and to a conventional infrared interferometer, which is used as a reference.

The infrared interferometer [see Fig. 2(c)] follows the classical scheme [1]. The optical path difference between the arms A1 and A2 is controlled by two all-fiber optical delay lines [16]. In this case the phase difference which is accumulated behind the telescopes T1 and T2 is  $\Delta \varphi + m(t)$  with  $\Delta \varphi$  being a constant bias. The two branches are recombined by another PM fiber coupler located right in front of an InGaAs photodetector. The differential fringe intensity is

$$dI_{\rm IR} = 2O(\theta) \{1 + \text{Re}[\exp\{j[2\pi\theta\xi + \Delta\varphi + m(t)]\}]\} d\theta$$
(2)

which yields a global intensity function

$$I_{\rm IR} = 2I_0[1 + |V(\xi)|\cos(\Delta\varphi + m(t) + \arg(V(\xi)))].$$
 (3)

In our setup we measure the fringe contrast at certain values of x, which are a multiple of the reference base b. The up-conversion interferometer [see Fig. 2(d)] basically follows the same interferometric scheme. Therefore, we can focus our discussion to the main difference which is the inclusion of an all-optical SFG element in each arm. Each wavelength converter consists of a 40 mm long Tiindiffused PPLN waveguide. They were fabricated by an indiffusion of 6  $\mu$ m wide, 55 nm thick Ti stripes into z-cut LiNbO<sub>3</sub> for 8.5 h at 1060 °C. The pooling period has been theoretically predicted by solving the Maxwell equations. The material dispersion has been modeled with the Sellmeier equation. We found that the ferroelectric domains should be inverted (poling) with a period of 11.30  $\mu$ m for phase-matched sum-frequency generation with a pump at 1064 nm and a signal at 1541 nm. The converters are individually temperature-stabilized to about 90 °C. Experiments were performed using a launched pump power of about 80 mW and a 1541 nm signal power of about 60 nW. The output power at 630 nm is in the range of 1 nW in the output monomode fibre. This means that the effective conversion efficiency, i.e., ratio of the SFG power in the output fiber to the launched signal power, is only about -18 dB. The theoretical conversion efficiency for the nonlinear process should be about -3 dB for 80 mW pump power. The discrepancy is mainly due to high coupling losses of the pump and signal waves into the waveguide and of the SF wave into the outgoing fiber. Therefore, a tremendous increase in the efficiency can be expected if the fiber-waveguide coupling is improved. Because of the crystal dispersion and length (40 mm), the conversion process is efficient in a band of 0.3 nm.

We combine the infrared signals coming from T1 or T2with the pump on each arm of the interferometer (fibers  $P_1$ and  $P_2$ ) by means of two PM fiber multiplexers. A precise control of the optical path difference between  $P_1$  and  $P_2$  is not required in our case, owing to the very large coherence length (hundreds of meters) of our single mode continous wave (CW) pump laser. As the two converters share the same pump, any eventual fluctuation of the pump phase is identically distributed in both arms of the interferometer and does not affect the phase difference. To isolate the SFG visible signal from other copropagating beams (pump, IR signal, pump frequency doubling in crystal) we used two identical interference filters (IF) of 20 nm FWHM centered at  $\lambda = 630$  nm. Consequently all optical elements behind the Ti:PPLN waveguides are conceived to work in the visible domain. The two optical fields are then coupled into two PM single mode optical fibers (bow tie)  $B_1$  and  $B_2$ , whose optical path difference is controlled by two PM allfiber delay lines in a push-pull configuration.

In the up-conversion interferometer, the origin of the phase difference is twofold. Similar to the infrared interferometer, a first contribution comes from the object position  $\theta$  and from the telescope separation  $\xi$ . This term provides a phase difference of  $2\pi\theta\xi$ . Note that although the interferometer operates in the visible domain, this contribution to the phase difference is entirely coming from the original infrared radiation. The phase difference is entirely copied when the carrier frequencies are upconverted with no loss of information as we have recently proved in Ref. [17].

The second contribution to the phase difference is due to the up-conversion process. An initial phase difference of the pump waves in the two converters is transferred to the SFG wave and, hence, results in a constant phase shift  $\Delta \varphi'$  in the interference signal. Therefore, the differential fringe intensity is given by

$$dI_{\text{vis}} = 2O(\theta) \{1 + \text{Re}[\exp\{j[2\pi\theta\xi + \Delta\varphi' + m(t)]\}]\} d\theta.$$
(4)

This results in the following fringe intensity function:

$$I_{\text{vis}} = 2I_0[1 + |V(\xi)|\cos(\Delta\varphi' + m(t) + \arg(V(\xi)))].$$
 (5)

Equations (3) and (5) show that, despite the presence of a possible phase offset, the fringe visibility function can be measured without any difference in both interferometers.

To prove our statement experimentally, we have carried out a series of measurements operating simultaneously the infrared and the up-conversion interferometers. The diamond marks of Fig. 3 report the fringe contrast that we

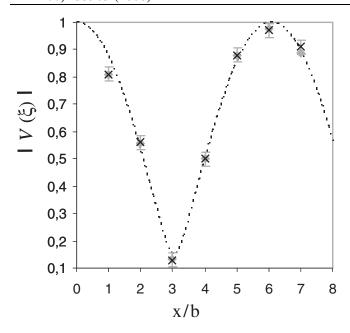


FIG. 3. Experimentally measured fringe contrast obtained from the up-conversion (crosses) and from the infrared interferometer (diamonds). The dashed curve shows our calculations assuming  $\theta_0=15~\mu {\rm rad}$ .

measured using our reference infrared interferometer and varying the telescope distance x by steps equal to b. Their trend clearly identifies a periodic function, whose period can give us the angular separation of the binary source. Note that these visibility measurements include the corrections of photometric and polarization imbalance. We have exploited such classical results of indirect imaging as a test bed for our interferometers. For comparison, the dashed line represents the contrast function that can be analytically calculated for the specific case of an angular distance  $\theta_0$  = 15  $\mu$ rad and an intensity ratio of 74% between the two sources. We have carried out the same set of measurements with our up-conversion interferometer. The crosses of Fig. 3 show the measured fringe contrast. The obtained fringe visibility (with fringes in the visible) is in perfect agreement with those obtained with the infrared interferometer (accuracy of 4%). For the sake of completeness, we only show the uncertainty bar associated with the upconversion interferometer.

In conclusion, we have carried out an experimental study of indirect imaging by using an up-conversion interferometer which transfers the coherence properties of an infrared source into the visible domain. The reliability of our results is confirmed by the comparison with results obtained with the reference interferometer in the infrared domain. The validity of the direct link between the intensity function of an object and the visibility function of fringes is preserved by introducing two wavelength conversion elements. Our measurements in the visible and infrared domains are in perfect agreement, and the upconversion interferometer allows us to retrieve the visibility of an infrared source by observing the interferometric signal in the visible domain. A drawback of the current upconversion interferometer is the limited spectral bandwidth of the wavelength converters determined by the requirement of phase matching. A broadening of the bandwidth might be achieved by chirping of the poling period along the waveguide. It is planned to study such converters with chirped poling structures and to extend the signal wavelength range further into the infrared.

- \*francois.reynaud@xlim.fr
- [1] P.R. Lawson, Selected Papers on Long Baseline Stellar Interferometry (SPIE Milestone Series, Washington, 1997).
- [2] A. Michelson, Astrophys. J. **51**, 257 (1920).
- [3] R. H. Brown et al., Nature (London) 177, 27 (1956).
- [4] M. A. Johnson et al., Phys. Rev. Lett. 33, 1617 (1974).
- [5] S. L. Jansen et al., J. Lightwave Technol. 24, 54 (2006).
- [6] M. Bellini et al., Appl. Phys. B 65, 677 (1997).
- [7] G. Perrin et al., Science 311, 194 (2006).
- [8] M. M. Abbas et al., Appl. Opt. 15, 961 (1976).
- [9] R. W. Boyd et al., Appl. Phys. Lett. 31, 440 (1977).
- [10] E. J. Lim et al., Appl. Phys. Lett. **59**, 2207 (1991).
- [11] M. A. Albota et al., Opt. Lett. 29, 1449 (2004).
- [12] A.P. VanDevender et al., J. Opt. Soc. Am. B 24, 295 (2007).
- [13] M. Born and E. Wolf, *Principles of Optics* (Pergamon Press, New York, 1980).
- [14] R. V. Roussev et al., Opt. Lett. 29, 1518 (2004).
- [15] J. Warner et al., Appl. Phys. Lett. 13, 360 (1968).
- [16] L. M. Simohamed et al., Pure Appl. Opt. 5, 1005 (1996).
- [17] L. Del Rio et al., Opt. Commun. 281, 2722 (2008).